AN M-BAND, 2-DIMENSIONAL TRANSLATION-INVARIANT WAVELET TRANSFORM AND APPLICATIONS

Stephen Del Marco, Peter Heller, and John Weiss

Aware, Inc.
One Memorial Drive
Cambridge, MA 02142 USA

ABSTRACT

This paper develops a two-dimensional M-band translation-invariant wavelet transform (2-d MTI). Use of the MTI overcomes the shift-variance of the wavelet transform by applying a cost function over M shifts of the input signal. The new transform is proven to be translation-invariant. Use of M-band wavelets enables a finer frequency partitioning and greater energy compaction in the transform representation. Examples are presented which show that the translation-invariant transforms provide superior energy concentration compared to the corresponding nominal wavelet transforms. Examples are also presented comparing the energy concentration capability of M-band wavelets and the Modulated Lapped Transform (MLT).

1. INTRODUCTION

Wavelet-related methods have seen much use in signal and image processing. However, M-band wavelet-related methods have been used less frequently. M-band wavelets [1, 2, 3] have been applied to image compression [1], transient signal detection [4], and texture analysis [5].

M-band wavelets have advantages over dyadic wavelets for certain applications. Among these advantages are a greater variety of practically implementable wavelets of compact support. The parameter space describing M-band wavelets is much richer than that in the 2-band case. M-band wavelets also more rapidly achieve a given frequency resolution as a function of decomposition scale. This provides greater freedom and flexibility in choosing time-frequency tilings.

Discrete wavelets and wavepackets have the disadvantage of being non-translation-invariant. This results from the decimation involved in performing the wavelet transform. To address this problem, a 2-d translation-invariant wavelet transform was developed in [6], based on the 1-d transform of Weiss [7].

This paper generalizes the 2-d transform to the M-band case (2-d MTI), and presents applications to image processing. We show that use of the MTI pro-

vides superior energy concentration over nominal wavelet methods. We also compare the performance of M-band wavelets with the Modulated Lapped Transform [8] as components of a translation-invariant wavelet transform for energy compaction.

This paper is organized as follows. Section 2 summarizes M-band wavelets, presents the 2-d MTI definition, and proves translation-invariance. Section 3 presents applications to image processing, and Section 4 presents conclusions.

2. THE 2-D, M-BAND TI

2.1 Two Dimensional, M-band Wavelets

Recall that the M-band wavelet and wave-packet transforms are formed by iterating an M-band paraunitary multirate filter bank. Such a filter bank is a collection of M filters a_i, $i = 0, 1, \ldots, M - 1$ with taps $a_{i,k}$, $k \in \{0, 1, \ldots, Mg-1\}$ satisfying the orthogonality conditions:

$$\sum_k a_{i,k+Ml} a_{i',k+Ml'} = M \delta_{i,i'} \delta_{l,l'}.$$

The genus $g = N/M$ (where N is the filter length), controls the overlap of the filters. Imposition of the d.c. condition:

$$\sum_k a_{i,k} = M \delta_{i,0}$$

distinguishes M-band wavelets from general M-channel paraunitary filterbanks.

The wavelet filter bank may satisfy a vanishing-wavelet-moment or "regularity" condition [2]; this is particularly useful when the filter bank is to be iterated in a wavelet decomposition. Alternatively, the filter bank may be derived from a lowpass prototype filter via cosine modulation [8]. The outputs of the filter bank are obtained by convolving an input signal with each of the M filters a_i and downsampling the output by a factor of M. This produces a critically sampled signal representation. When iterated in a tree structure, a wavelet [9] or wave-packet [10] representation results.

Extend the 1-d filtering operations

$$F_{\alpha,i}(s) = \sum_n s_n a_{i,Mk-n}, \quad \alpha \in \{x, y\}$$

to 2-d, through tensor products:

$$F_{i,j} = F_{y,i} \otimes F_{x,j}, \quad i,j \in \{0, \dots, M-1\}.$$

These filtering operations consist of filtering in the x direction with filter a_j, downsampling by a factor of M, followed by filtering these sequences in the y direction with filter a_i and downsampling by a factor of M.

The single level M-band wavelet decomposition is given by $F = F_{0,0} \times \dots \times F_{M-1,M-1}$. The complete M-band wavelet transform is obtained by iteration on the lowpass band.

2.2 Definitions

Let $\mathcal{S}_x, \mathcal{S}_y$ represent the unit periodic shift operators in the x and y directions. That is, for $s(\xi, \eta) \in \mathbf{R}^m \times \mathbf{R}^m$, with $\xi, \eta \in \{0, 1, \dots, m-1\}$

$$\mathcal{S}_x s(\xi, \eta) = s(\xi+1, \eta), \quad \mathcal{S}_y s(\xi, \eta) = s(\xi, \eta+1)$$

where the addition is performed mod m. Let Z_M denote the M-element finite set $\mathbf{Z}/M = \{0, 1, \dots, M-1\}$. Define a generalized notion of a translation-invariant operator T, applied to an image $s(\xi, \eta)$ as

$$T\mathcal{S}_x^p \mathcal{S}_y^q(s) = \mathcal{S}_x^k \mathcal{S}_y^l T(s), \quad k,l \in \{0, 1\}, \quad p,q \in Z_M,$$

with $(p, q) \neq (0, 0)$. This definition means that any combination of shifts in the x or y directions by amounts between 0 and $M-1$, results in some combination of transform shifts by 0 or 1. Let C denote an additive cost function [10], defined on images of arbitrary size.

The 2-d MTI consists of performing transforms of M shifts of the input image, and choosing the coefficient set which minimizes the cost function. Let F^{TI} denote the 2-d MTI, then for $k, l \in Z_M$

$$F^{TI}(s) = F\mathcal{S}_x^k \mathcal{S}_y^l(s) \quad \text{if} \quad C(F\mathcal{S}_x^k \mathcal{S}_y^l(s)) = C_{min}$$

for

$$C_{min} = \min_{p,q}\{C(F\mathcal{S}_x^p \mathcal{S}_y^q(s)), \quad p,q \in Z_M\}.$$

The definition is subject to the constraint:

$$C(F\mathcal{S}_x^i \mathcal{S}_y^j(s)) \neq C(F\mathcal{S}_x^p \mathcal{S}_y^q(s)). \tag{1}$$

where

$$i,j,p,q \in Z_M, \quad (i,j) \neq (p,q).$$

The constraint may be removed, and the definition may be generalized as in [6]. However, this constraint is usually realized in practical applications.

Note that the MTI differs from the shift-invariant wavelet transform defined in [11]. They achieve shift-independence by performing the full wavelet decomposition for *all* shifts of the input signal and choosing the minimal cost transform coefficient set. The MTI performs M shifts at *each* decomposition level.

2.3 Translation-Invariance Proof

The proof requires the following lemma:

Lemma 1 *for* $\alpha \in \{x, y\}$

$$F\mathcal{S}_\alpha^M(s) = \mathcal{S}_\alpha F(s), \quad \mathcal{S}_x^i \mathcal{S}_y^j(s) = \mathcal{S}_y^j \mathcal{S}_x^i(s), \quad \text{and}$$
$$C(\mathcal{S}_\alpha F(s)) = C(F(s)).$$

The lemma states that shifts by M of the image, produce shifts by 1 in the transform coefficients, shifts commute, and the additive cost function is independent of shifts of the input image.

The translation-invariance properties of the 2-d MTI are contained in the following theorem:

Theorem 1 *For $p, q \in Z_M$ subject to the constraint (1), there exists $u, v \in \{0, 1\}$ such that*

$$F^{TI}\mathcal{S}_x^p \mathcal{S}_y^q(s) = \mathcal{S}_x^u \mathcal{S}_y^v F^{TI}(s).$$

Proof

Assume the minimum cost over the various shifts, is $C(F\mathcal{S}_x^r \mathcal{S}_y^j(s))$. Then by definition $F^{TI}(s) = F\mathcal{S}_x^r \mathcal{S}_y^j(s)$. Consider a shift of s by $\mathcal{S}_x^p \mathcal{S}_y^q$. Then by definition, for some $k, l \in Z_M$, $F^{TI}\mathcal{S}_x^p \mathcal{S}_y^q(s) = F\mathcal{S}_x^{k+p} \mathcal{S}_y^{l+q}(s)$. Now, take k, l such that $k + p \equiv r \bmod M$, $l + q \equiv j \bmod M$. These relations imply the existence of $u, v \in \{0, 1\}$ such that $k + p = r + Mu$, $l + q = j + Mv$. Substitution gives

$$\begin{aligned} F^{TI}\mathcal{S}_x^p \mathcal{S}_y^q(s) &= F\mathcal{S}_x^{r+Mu} \mathcal{S}_y^{j+Mv}(s) \\ &= \mathcal{S}_x^u \mathcal{S}_y^v F\mathcal{S}_x^r \mathcal{S}_y^j(s). \end{aligned}$$

Hence

$$\begin{aligned} C(F^{TI}\mathcal{S}_x^p \mathcal{S}_y^q(s)) &= C(\mathcal{S}_x^u \mathcal{S}_y^v F\mathcal{S}_x^r \mathcal{S}_y^j(s)) \\ &= C(F\mathcal{S}_x^r \mathcal{S}_y^j(s)) \\ &= C_{min}, \end{aligned}$$

which implies

$$F^{TI}\mathcal{S}_x^p \mathcal{S}_y^q(s) = \mathcal{S}_x^u \mathcal{S}_y^v F\mathcal{S}_x^r \mathcal{S}_y^j(s)$$

Thus

$$F^{TI}\mathcal{S}_x^p \mathcal{S}_y^q(s) = \mathcal{S}_x^u \mathcal{S}_y^v F^{TI}(s).$$

Remark 1 *For M-bands, calculation of the MTI requires calculating the single level M-band wavelet transform for M^2 image shifts. The computational complexity is $O(n^2)$ for a size $n \times n$ image, but may become computationally intensive for large M. However, the algorithm is almost completely parallelizable.*

Remark 2 *Assume $M = 2^L$, and consider a square image each side of length M^N. Then, $M^N = 2^{LN}$. Hence, to perform a complete wavepacket decomposition, L times more decomposition levels are required for the 2-band case, than for the M-band case.*

Remark 3 *Let $G(\mathcal{S}_x, \mathcal{S}_y)$ be the group of shift operators of the form $\mathcal{S}_x^p \mathcal{S}_y^q$ for $p, q \in Z_M$. Then $G(\mathcal{S}_x, \mathcal{S}_y) = G(\mathcal{S}_x) \otimes G(\mathcal{S}_y)$. That is, the group of shifts of the form $\mathcal{S}_x^p \mathcal{S}_y^q$ may be viewed as the tensor product of cyclic groups generated by $\mathcal{S}_x$ and $\mathcal{S}_y$. Then, the MTI may be modified by considering choices of shifts drawn from some subgroup $H(\mathcal{S}_x, \mathcal{S}_y) \subset G(\mathcal{S}_x, \mathcal{S}_y)$ with $H(\mathcal{S}_x, \mathcal{S}_y) = H(\mathcal{S}_x) \otimes H(\mathcal{S}_y)$, for $H(\mathcal{S}_\alpha) \subset G(\mathcal{S}_\alpha)$. Hence, the MTI will be shift-invariant on shifts drawn from $H(\mathcal{S}_x, \mathcal{S}_y)$. This formulation provides a trade-off between computational complexity and degree of shift-invariance.*

Remark 4 *The theory developed here may be applied to definition of a wavelet transform, independent on operators $x_i \in G$, a finite group. To see this, define*

$$F^G(s) = F x_j(s)$$

if

$$C(F x_j(s)) = \min_i \{C(F x_i(s)), \; x_i \in G\}.$$

Then, for any $x_k \in G$, it is easy to show $F^G x_k(s) = F x_j(s)$. Note that the transform in [11] is an example of such a transform.

3. APPLICATION TO IMAGE PROCESSING

We explored the MTI as a tool for image processing by using it to represent several different images. For each image, we retained a small subset of the MTI coefficients, then reconstructed and measured the reconstruction error of this reduced or smoothed version of the image. In the examples to follow, we plot normalized MSE against the number of highest energy terms retained. These curves correspond to rate-distortion curves, for a simple compression scheme based on retaining a fixed number of highest energy terms. The number of terms retained is directly proportional to compression ratio for this thresholding scheme. We compare its performance with analogous schemes based on the nominal M-band wavelet transform (MWT).

In general, the MTI should provide a lower-entropy representation for images. This results from the entropy minimization performed in the MTI, over several shifts of the input image. At each level, those transform coefficients are retained which provide minimum entropy.

Figure 1 contains a 128 by 128 bi-level newspaper headline image. Figure 2 contains the MSE curves, and shows superior representation performance of the MTI over the MWT. A 4-band, genus 2, 2-vanishing moment wavelet filter has been used [1].

The superior performance is indicated by a lower MSE for a fixed number of retained coefficients. Alternatively, superior performance may be measured by a smaller number of retained coefficients for reconstruction to a fixed MSE. Figure 2 shows a maximum performance improvement of over 31%. The MTI appears
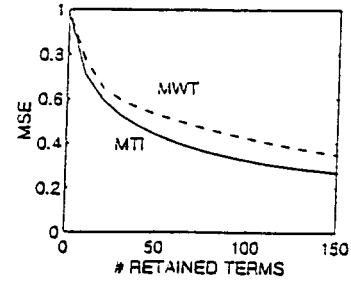

Figure 1: Bi-Level Headline Image

Figure 2: MSE Curves for Headline Image

to work well for imagery which exhibits sharp discontinuities (e.g. bi-level imagery). For smooth imagery, the performance is not as striking. However, small improvement may be obtained for a region of compression ratios. As an example, Figure 3 contains a 128 by 128 center section zoom of the Lena image. Figure 4 contains the MSE curves, for a small region of compression ratios. Figure 4 shows a maximum performance improvement of just over 13%.

The MTI can also work well for data exhibiting high dynamic range. Figure 5 contains MSE curves for a 128 by 128 sample of seismic imagery (not shown). The flexibility of M-band wavelets is exploited here by using a custom designed wavelet lowpass filter with three vanishing moments, and additional double zeros at $\omega = \frac{3\pi}{4}, \frac{5\pi}{4}$ [12]. Again, the MTI shows a performance improvement over the MWT.

We also compare the performance of the MTI for higher genus wavelet filters, and M-band Modulated Lapped Transforms [8] of the same genus. We compare the genus 4 wavelet and MLT filter banks, des-

Figure 3: Portion of Lena Image
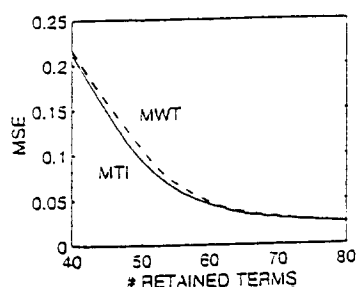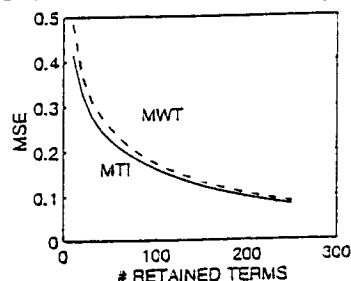
Figure 4: MSE Curves for Lena Image Portion

Figure 5: MSE Curves for Seismic Image

ignated respectively as M4n4 and M4n2_mlt, and the genus 2 wavelet and MLTs, designated respectively as M4n2 and M4n2_mlt. Figure 6 contain the MSE curves, for the bi-level newspaper headline image (Figure 1). Figure 6 indicates that the genus 2 filters outperform the genus 4 filters at the lower compression ratios. This seems natural, since the genus two filters are shorter and therefore better able to capture the sharp discontinuities in the bi-level imagery. Furthermore, higher genus wavelets offer higher orders of polynomial interpolation [2], which are unnecessary for the bi-level image. At high compression ratios, the Malvar filters provide a performance advantage over the M-band wavelets.

4. CONCLUSIONS

A 2-d, M-band translation-invariant wavelet transform was presented and proven to be translation-invariant. MSE curves were presented, comparing reconstructions using the MTI and MWT for the Lena image, a bi-level newspaper headline image, and sample seismic data. Genus 2 and 4 wavelet filters were compared with Modulated Lapped Transforms. Results indicated that su-
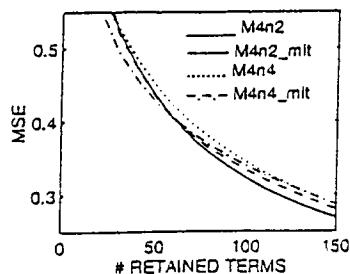

Figure 6: MSE Curves for Wavelet and MLT filters

perior compression was obtained using the MTI for the bi-level and seismic images. An improvement in compression was also obtained for the Lena image, for a small interval of compression ratios.

5. References

[1] P. N. Heller and H. L. Resnikoff, "Regular M-Band Wavelets and Applications", *Proc. of IEEE ICASSP*, vol. **III**, pp. 229-232, 1993.

[2] P. Steffen, P. N. Heller, R. A. Gopinath and C. S. Burrus, "Theory of Regular M-Band Wavelet Bases", *IEEE Trans. on Sig. Proc.*, vol. SP-41, no. 12., pp. 3497-3511, Dec. 1993.

[3] H. Zou and A. H. Tewfik, "Discrete Orthogonal M-Band Wavelet Decompositions," *Proc. IEEE ICASSP*, vol. **IV** , pp. 605-608, 1992.

[4] S. Del Marco and J. Weiss, "M-Band Wavepacket-Based Transient Signal Detector Using a Translation-Invariant Wavelet Transform", *Optical Eng.* vol. 33, no. 7, pp. 2175-2182, July 1994.

[5] T. Greiner, J.-P. Casel and M. Pandit, "Texture Analysis with a Texture Matched M-Channel Wavelet Approach", *Proc. IEEE ICASSP*, vol **V**, pp. 129-132, 1993.

[6] S. Del Marco and J. Weiss, "Applications of a 2-D Translation-Invariant Wavepacket Transform to Image Processing", *submitted to IEEE Sig. Proc. Lett.*

[7] J. Weiss, "Translation-Invariance and the Wavelet Transform," *Aware Tech. Rept.* no. AD921102, 1993.

[8] H. S. Malvar, *Signal Processing with Lapped Transforms*, Norwell, MA: Artech House, 1992.

[9] S. Mallat, "A Theory for Multiresolution Signal Decomposition: The Wavelet Representation", *IEEE Pat. Anal. and Mach. Intel.*, vol PAMI-11, no. 7, pp. 674-693, July 1989.

[10] R. R. Coifman and M. V. Wickerhauser, "Entropy-Based Algorithms for Best-Basis Selection", *IEEE Trans. on Inform. Theory*, vol. IT-38, no. 2, pp. 713-718, March 1992.

[11] J. Liang and T. W. Parks, "A Two-Dimensional Translation Invariant Wavelet Representation and Its Applications", *Proc. of IEEE ICIP*, vol. **I**, pp. 66-70, 1994.

[12] P. N. Heller, "Lagrange M-th Band Filters and the Construction of Smooth M-Band Wavelets" *Proc. of IEEE-SP Int. Symp. on Time-Freq. and Time-Scale Anal.*, pp. 108-111, 1994.